Since January 2020 Elsevier has created a COVID-19 resource centre with free information in English and Mandarin on the novel coronavirus COVID-19. The COVID-19 resource centre is hosted on Elsevier Connect, the company's public news and information website.

Elsevier hereby grants permission to make all its COVID-19-related research that is available on the COVID-19 resource centre - including this research content - immediately available in PubMed Central and other publicly funded repositories, such as the WHO COVID database with rights for unrestricted research re-use and analyses in any form or by any means with acknowledgement of the original source. These permissions are granted for free by Elsevier for as long as the COVID-19 resource centre remains active.

Knowledge-Based Systems 258 (2022) 110040

Contents lists available at ScienceDirect

Knowledge-Based Systems

journal homepage: www.elsevier.com/locate/knosys

BND-VGG-19: A deep learning algorithm for COVID-19 identification utilizing X-ray images

Zili Cao [a], Junjian Huang [a,*], Xing He [a], Zhaowen Zong [b]

[a] Chongqing Key Laboratory of Nonlinear Circuits and Intelligent Information Processing, College of Electronic and Information Engineering, Southwest University, Chongqing 400715, PR China
[b] Department of Training Base for Health Care, Army Medical University, Chongqing 400038, PR China

ARTICLE INFO

Article history:
Received 27 July 2022
Received in revised form 9 October 2022
Accepted 14 October 2022
Available online 21 October 2022

Keywords:
COVID-19
VGG-19
X-ray image
Classification
Diagnosis

ABSTRACT

During the past two years, a highly infectious virus known as COVID-19 has been damaging and harming the health of people all over the world. Simultaneously, the number of patients is rising in various countries, with many new cases appearing daily, posing a significant challenge to hospital medical staff. It is necessary to improve the efficiency of virus detection. To this end, we combine modern technology and visual assistance to detect COVID-19. Based on the above facts, for accurate and rapid identification of infected persons, the BND-VGG-19 method was proposed. This method is based on VGG-19 and further incorporates batch normalization and dropout layers between the layers to improve network accuracy. Then, the COVID-19 dataset including viral pneumonia, COVID-19, and normal X-ray images, are used to diagnose lung abnormalities and test the performance of the proposed algorithm. The experimental results show the superiority of BND-VGG-19 with a 95.48% accuracy rate compared with existing COVID-19 diagnostic methods.

© 2022 Elsevier B.V. All rights reserved.

1. Introduction

Because of the outbreak of the new coronavirus COVID-19 in the past two years, people's physical health worldwide has been seriously affected. As the World Health Organization (WHO) COVID-19 study [1] officially announced, COVID-19 is a severe acute respiratory syndrome coronavirus 2 (SARS-CoV-2) that can cause acute respiratory infections. Medical imaging such as X-rays and computed tomography (CT) scans are critical in the global effort against COVID-19. Artificial intelligence could improve efficiency by correctly showing infections in X-ray and CT images, and computer-aided systems could help doctors make clinical judgments, such as disease diagnosis. However, many research classifications on COVID-19 are specific to binary types, which are not rigorous enough for modern medicine. Most of the training data of them are supported by a large amount of dataset. When a new virus strikes, the problem of lack of data for training is faced. Dealing with an emerging situation with little data collection to analyze, issues such as under-fitting and insufficient generalization ability was arising, leading to the risk of inaccurate identification. Therefore, this paper proposes a method suitable for triple classification, which is ideal for few and unbalanced data. The feature is to add BN (Batch Normalization) and Dropout layers based on the original VGG-19 and try different parameters to get the best experimental results and then the best network structure. In comparative experiments, we add the BN layer and Dropout layer to the VGG-16 model and try different parameter variations, and it consistently outperforms the test set on the training set. At the same time, the experimental results of VGG-19 without a BN layer or Dropout layer are compared. Finally, the test data results of all experiments are given and compared. The experimental results show that, in this case, the BND-VGG-19 method could classify and detect chest X-ray images well.

Our main contributions are presented as follows:

- A classification deep learning algorithm, BND-VGG-19, is proposed for small and imbalanced datasets.
- The introduced algorithm BND-VGG-19 is to identify X-ray images for COVID-19.

In detail, this paper presented the computational model and experiments, organized as follows. Section 2 provides an overview of general detection measures for COVID-19 and related research. The proposed network structure is detailed in Section 3. The associated experiments and data are in Sections 4–5. Section 6 summarizes future research work and conclusions.

* Corresponding author.
E-mail address: hmomu@sina.com (J. Huang).

https://doi.org/10.1016/j.knosys.2022.110040
0950-7051/© 2022 Elsevier B.V. All rights reserved.

2. Related work

2.1. Diagnosis of COVID-19

The latest measure of COVID-19, reverse transcription polymerase chain reaction (RT-PCR), is to collect a specimen of people's upper respiratory tract, then test by professional laboratory equipment. Initially, patients are unaware of being infected, which leads to a significant risk of contagion to the surroundings. In addition, the RT-PCR approach cannot determine the severity of the disease, since it requires the diagnosis of specialized medical experts, which is tricky and time-consuming. X-ray imaging is a simple method that can accurately identify COVID-19-positive patients and is crucial in determining the severity of respiratory issues. Besides, the sensitivity of chest imaging for COVID-19 was officially recognized as an effective screening technique for diagnosing pneumonia [2]. Ai et al. [3] pointed out that medical scanning chest pictures can be employed to identify COVID-19 clinically. Chest X-ray, chest CT and ultrasound were demonstrated to be applicable in case management and screening procedures by examining respiratory preferences for COVID-19. Most detection techniques are based on X-ray or CT images. X-ray images are a priority at this stage because they are well suited for diagnostic purposes and easy to perform. Chest CT scans are not as readily available as X-ray images, and they are more expensive and harmful than X-ray images from an economic and radiation dose perspective. Therefore, chest X-ray images are used in this study.

2.2. Classification of COVID-19

Li et al. [4] proposed an efficient mining algorithm called Nettree for NMSP Mining (NetNMSP), which has three key steps: computing support, generating candidate patterns, and determining NMSP. NMSP and frequent patterns could be mined in SARS-CoV-1, SARS-CoV-2, and MERS-CoV to distinguish differences among viral sequences. Ozturk et al. [5] began with the Darknet-19 model and progressively increased the number of filters to 8, 16, and 32. Furthermore, 17 convolutional layers were added to the proposed model. Each DN (Darknet) layer starts with a convolutional layer followed by Batch Norm and LeakyReLU operations, while each 3 Conv layer repeats the same settings three times in a sequential manner. Sethy et al. [6] proposed a deep learning-based technique for detecting coronavirus-infected individuals using X-ray pictures. The support vector machine classifies X-ray pictures from other coronavirus-affected images using depth characteristics. That is resnet50 plus the SVM-achieved accuracy. Wu et al. [7] introduced the OPP-Miner algorithm to mine patterns with the same trend (subsequence with the same relative order). The algorithm has high utility in analyzing the COVID-19 epidemic by identifying key trends and improving clustering performance. Pereira et al. [8] provided a classification approach incorporating multi-class and hierarchical categorization. In the model, early and late fusion strategies are investigated to use numerous texture descriptors and the underlying classifier simultaneously. For COVID-19 detection, Ashour et al. [9] developed an ensemble-based BoF classification algorithm. Integration is offered in this model for the BoF classification stage. The method is evaluated and compared to other categorization systems for various numbers of visual words. Widodo et al. [10] used three architectural layers in their deep learning system (UBNet v3). Initially, an architecture with seven convolutional and three ANN layers (UBNet v1) is built to discriminate between normal and pneumonia pictures. Secondly, pictures of bacterial and viral pneumonia are classified using four layers of convolution and three layers of ANN (UBNet v2). Finally, UBNet v1 is applied to differentiate images of patients infected with the COVID-19 virus from those images infected with pneumonia virus. Yousri et al. [11] offered to use the updated cuckoo search optimization algorithm (CS) that used fractional-order calculus (FO), and four independent heavy-tailed distributions are recommended instead of Levy flights. All of these used the Mittag-Leffler distribution, Corsi distribution, Pareto distribution, and Weibull distribution. The proposed FO-CS version is validated using 18 UCI datasets as the first series of studies. Toraman et al. [12] proposed a unique neural network-based convolutional CapsNet to identify the COVID-19 virus utilizing chest X-ray images and a capsule network. Das et al. [13] developed an Inception Net for detecting New Hall pneumonia infection. Their model is shortened at the point where three Inception modules and one element size block are kept from the start, and then maximum pooling and global average pooling layers are cascaded to minimize the output dimension. Experimentation is used to choose the truncation points that produced the best categorization results. The work of Hasan et al. [14] employed preprocessing to reduce the effect of intensity fluctuations between CT slices. The background of CT lung images is separated using a histogram threshold, and feature extraction is performed for each CT lung scanning. The collected features are classified using a Long Short Term Memory (LSTM) neural network classifier.

Sun et al. [15] used three convolutional neural networks (LeNet-5, VGG-16, and ResNet-18) as the basic classification model for chest X-ray image detection of COVID-19, normal, and pneumonia. The accuracy and precision of LeNet-5, VGG-16, and ResNet-18 are improved after optimizing the model's hyperparameters using a biogeographic-based philosophy. Apostolopoulos et al. [16] performed only transfer learning on VGG19. The study by Horry et al. [17] was performed based on VGG-16 and VGG-19 using transfer learning and fine-tuning, respectively.

The abovementioned are some methods of classification of COVID-19, but most of them are for binary classification. Nevertheless, COVID-19 is three classifications, which shows that it is insufficient from a medical point of view. At the same time, the datasets used in these methods are balanced with the mass of data. However, for an emerging virus, the data at their disposal was limited. A deficient and imbalanced dataset could replicate the data models in the face of a new unknown virus. Therefore, our proposed method concerning three classifications of COVID-19 used an inherently deficient and imbalanced dataset.

3. Materials & Methods

3.1. BN (Batch Normalization)

Ioffe et al. [18] proposed a new mechanism called Batch Normalization, which reduced the variation in the distribution of nodes within a deep network, sped up the training of neural networks, and made it possible to use saturated non-linear by reducing the dependence of gradients on parameter size or initial values, in addition to Batch Normalization by preventing the network from falling into saturated patterns. Firstly, the BN layer calculates the sample mean and variance and normalizes the sample data. Then, two parameters γ and β were introduced to perform the translation and scaling. The network trains, learns, and reconstructs the two parameters γ and β through the BN layer and learns its feature distribution. Therefore, including BN layers could speed up training, allow the network to be trained with a higher learning rate, improve the generalization ability of the network, and allow for shuffling the order of training samples (so that it is impossible to select the same photo multiple times for training). Thereby, the accuracy of the network could be improved.

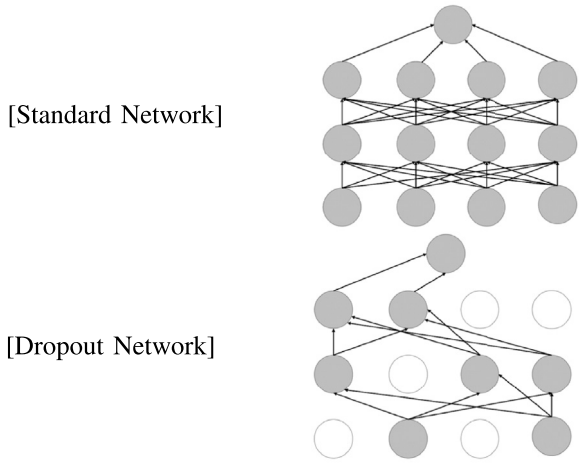

Fig. 1. Network structure.

Fig. 2. CVOID-19 dataset (From left to right: COVID-19, viral pneumonia, Normal).

3.2. Dropout

A Dropout technique was introduced by Srivastava et al. [19]. Dropout is a strategy for dealing with over-fitting by mixing predictions from several different large neural networks at the test. Because of the slow training speed of the complex network, it is challenging to mix predictions from separate large neural networks to combat over-fitting. During deep learning network training, neural network units are randomly and briefly popped out of the network with a fixed probability. Dropout is unpredictable training for each mini-batch is a new network and only temporary for stochastic gradient descent. Time-consuming and prone to over-fitting is an intractable problem in most networks. Dropout solves the over-fitting problem by changing the previous network to a slimmer one, as shown in Fig. 1 below.

3.3. COVID-19 dataset

Pavlova et al. [20] created the dataset using COVID-19 X-ray imaging data from the Italian Society of Medical, Interventional Radiology (SIRM) and the Novel Coronavirus 2019 dataset, including 43 different studies. This paper uses 219 COVID-19 chest X-ray images, 1341 normal images, and 1345 viral pneumonia images. All those are in Portable Network Graphics (PNG) format with 1024*1024 pixels, which can be easily converted to the required pixels for popular Convolutional Neural Networks (CNN), as illustrated in Fig. 2. In our experiments, we train a total of 4790 chest X-ray images divided into three groups. Meanwhile, as shown in Table 1, 80% COVID-19 dataset as the training dataset and 20% COVID-19 dataset as the validation set for training are categorized.

Table 1
The arrangements of datasets.

Class	COVID-19	Health	Pneumonia	Total
Train	175	1040	1040	2255
Validation	44	260	260	2132
Total	219	1300	1300	4790

Table 2
VGG-16 Network structure.

NO.	Layers	Type	0utput
1	2D Convolution_1 of Block_1	3 × 3	64, 224, 224
2	2D Convolution_2 of Block_1	3 × 3	64, 224, 224
Max pool			
3	2D Convolution_1 of Block_2	3 × 3	128, 112, 112
4	2D Convolution_2 of Block_2	3 × 3	128, 112, 112
Max pool			
5	2D Convolution_1 of Block_3	3 × 3	256, 56, 56
6	2D Convolution_2 of Block_3	3 × 3	256, 56, 56
7	2D Convolution_3 of Block_3	3 × 3	256, 56, 56
Max pool			
8	2D Convolution_1 of Block_4	3 × 3	512, 28, 28
9	2D Convolution_2 of Block_4	3 × 3	512, 28, 28
10	2D Convolution_3 of Block_4	3 × 3	512, 28, 28
Max pool			
11	2D Convolution_2 of Block_5	3 × 3	512, 14, 14
12	2D Convolution_3 of Block_5	3 × 3	512, 14, 14
13	2D Convolution_4 of Block_5	3 × 3	512, 14, 14
Max pool			
14	FC1	Fully connected	4096
15	FC2	Fully connected	4096
16	FC3	Fully connected	1000
Soft max			

3.4. VGG

Simonyan and Zisserman [21] devised the VGG deep convolutional neural network model, which got its name from the acronym of the author's research group at the University of Oxford. VGG adopts a deeper network topology and smaller convolution kernels to ensure the perceptual field of view. In convolutional layers, the number of variables is minimized. Smaller pooling kernels enable more comprehensive data collection. More channels can extract more information, VGG has six different network structures, but each group contains five groups of convolutions. Each group uses 3 × 3 convolution kernel size '1' and '0' padding, where each followed by 2 × 2 max pooling with stride 2, followed by three fully connected layers. The first layer of the VGG network has 64 channels, and each subsequent layer is doubled to a maximum of 512 channels. VGG-19 contains nineteen layers, and VGG-16 contains sixteen layers divided into a total of five blocks by a max pooling layer. Their structure diagrams are shown in Tables 2 and 3.

3.5. BND-VGG-19

For an emerging virus, the available data is limited, which means that the dataset is small and unbalanced. The VGG model has a relatively deep network structure, a smaller convolution kernel, and a pooling sampling domain. It can control the number of parameters while obtain more image features, avoid over-computation and over-complex structures. According to the dataset's characteristics, a BN layer was added to the network. The problem of increased learning difficulty caused by the distribution of distinct layers during the training process could be alleviated. It can speed up the training and convergence of

Table 3
VGG-19 Network structure.

NO.	Layers	Type	Output
1	2D Convolution_1 of Block_1	3 × 3	64, 224, 224
2	2D Convolution_2 of Block_1	3 × 3	64, 224, 224
Max pool			
3	2D Convolution_1 of Block_2	3 × 3	128, 112, 112
4	2D Convolution_2 of Block_2	3 × 3	128, 112, 112
Max pool			
5	2D Convolution_1 of Block_3	3 × 3	256, 56, 56
6	2D Convolution_2 of Block_3	3 × 3	256, 56, 56
7	2D Convolution_3 of Block_3	3 × 3	256, 56, 56
8	2D Convolution_4 of Block_3	3 × 3	256, 56, 56
Max pool			
9	2D Convolution_1 of Block_4	3 × 3	512, 28, 28
10	2D Convolution_2 of Block_4	3 × 3	512, 28, 28
11	2D Convolution_3 of Block_4	3 × 3	512, 28, 28
12	2D Convolution_4 of Block_4	3 × 3	512, 28, 28
Max pool			
13	2D Convolution_1 of Block_5	3 × 3	512, 14, 14
14	2D Convolution_2 of Block_5	3 × 3	512, 14, 14
15	2D Convolution_3 of Block_5	3 × 3	512, 14, 14
16	2D Convolution_4 of Block_5	3 × 3	512, 14, 14
Max pool			
17	FC1	Fully connected	4096
18	FC2	Fully connected	4096
19	FC3	Fully connected	1000
Soft max			

Table 4
Precision, Recall, based on BND-VGG-19.

	Precision	Recall
COVID-19	0.83	0.82
Normal	0.95	0.90
Vail pneumonia	0.90	0.91

the network and, further, prevent the gradient from exploding. Meanwhile, the decay learning rate is configured to improve the generalization ability of the entire network. Dropout forces a neural unit to work with other randomly selected neural units to significant effect. Therefore, the method of adding dropout layers is applied to remove the joint fitness between neuron nodes, enhance the generalization ability and reduce over-fitting.

Hence, a BN layer is inserted after each convolution kernel. A dropout layer is added after each module and each fully connected layer. In the VGG-19 network, without calculating the fully connected layer, the max-pool layer is used as the dividing line, and the remaining sixteen layers of the network are categorized into five blocks. Two convolutional layers and one pooling layer constitute the first two blocks, while four convolutional layers and one pooling layer constitute the last three modules. The network is then adjusted as described above; as shown in Fig. 3, Block-1 and Block-2 consist of two convolutional layers, two BN layers, one pooling layer, and one dropout layer; in Fig. 4, Block-3, Block-4, and Block-5 each has four convolutional layers, four BN layers, one pooling layer, and one dropout layer. Fig. 5 shows the overall network model of BND-VGG-19.

4. Experiments and results

4.1. Experiment A

A VGG19 model with a BN-only layer added is used to classify X-ray photographs into three groups: COVID-19, viral pneumonia, and normal. When using Relu as the activation function, the batch size is 32, and the epoch is 40. Train with two GPUs. The validation accuracy obtained for the VGG19 model with a BN-only layer added is 0.82, and its validation loss is 0.44. The results are listed in Table 5.

Table 5
The accuracy and loss.

	BN-only	Dropout-only	VGG16+BN+Dropout	BND-VGG-19
Val accuracy	0.8271	0.4517	0.8110	0.9548
Val loss	0.4455	0.8941	1.4384	0.1888

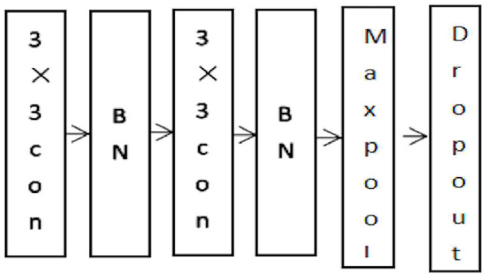

Fig. 3. Block-1 and Block-2 of BND-VGG-19.

4.2. Experiment B

A VGG-19 model with a Dropout-only layer added is used to classify X-rays into three groups: COVID-19, viral pneumonia, and normal. When using Relu as an activation function, Dropout = 0.1, Batch Size is 32, and epoch is 45. Train with two GPUs. The validation accuracy obtained for the VGG-19 model with a Dropout-only layer added is 0.40, and its validation loss is 0.89. The results are listed in Table 5.

4.3. Experiment C

The VGG-16 model with added BN layer and Dropout layer is used to classify X-ray photos into COVID-19, viral pneumonia, and normal. When using Relu as an activation function, Dropout is 0.1, Batch Size is 32, and epoch is 40. The validation accuracy obtained for the VGG-16 model with added BN layer and Dropout layer is 0.81, and its validation loss is 1.43. The results are listed in Table 5.

4.4. Experiment D

The BND-VGG-19 model is used to classify chest X-ray images into three groups: COVID-19, viral pneumonia, and normal. Relu is used as the activation function in the training process. The Dropout is 0.1, the learning rate is set to update dynamically, the Batch Size is 32, and the epoch is 40. It takes two GPUs to train in total. The validation accuracy obtained by BND-VGG-19 is 0.95, and the validation loss is 0.18, in Table 5. The results of training the curve of accuracy and loss values are shown in Fig. 6. The precision and recall are displayed in Table 4.

5. Evaluation & Discuss

5.1. Evaluation

In the evaluation, the accuracy value (ACC), precision value, and recall rate are provided, and their formulas are given. TP means that the positive class is predicted to be positive, TN means that the negative class is predicted to be negative, FP means that

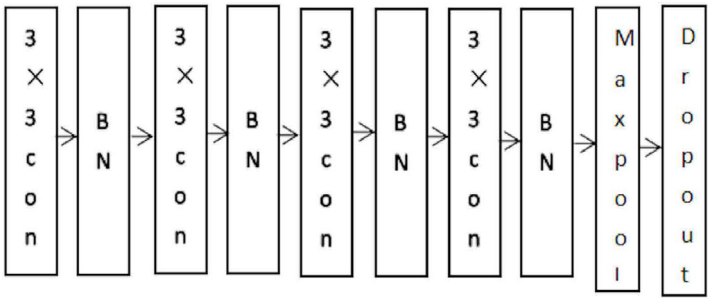

Fig. 4. Block-3, Block-4 and Block-5 of BND-VGG-19.

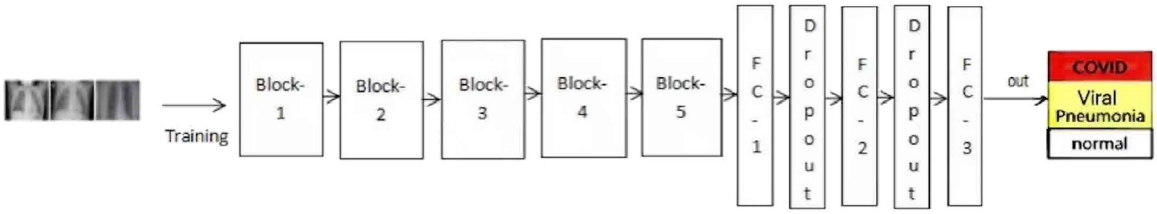

Fig. 5. BND-VGG-19.

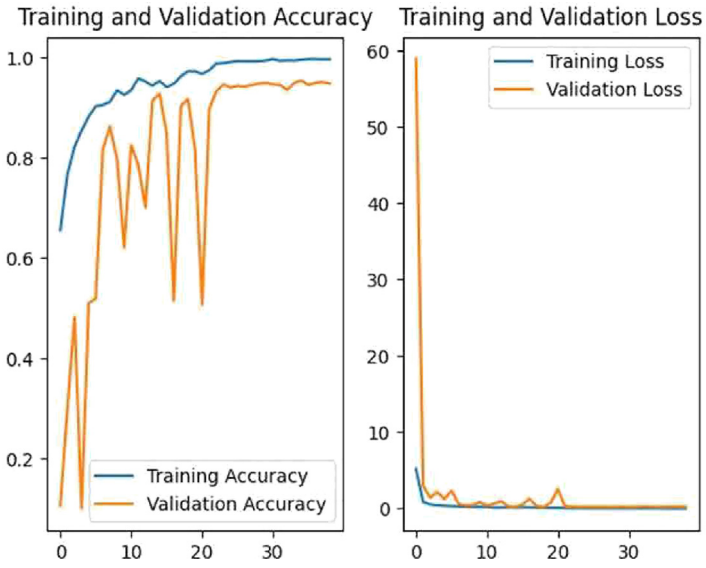

Fig. 6. The accuracy and loss of BND-VGG-19.

the negative class is predicted to be positive, and FN means that the positive class is predicted to be a negative class.

$$ACC = \frac{TP + TN}{TP + TN + FP + FN} \tag{1}$$

$$Precision = \frac{TP}{TP + FP} \tag{2}$$

$$Recall = \frac{TP}{TP + FN} \tag{3}$$

Then we compare the results of this work with other existing methods. Table 6 compares the experimental results of all three classes of networks using VGG as the base model. In Table 7, the results of different algorithms for triple classification are presented.

5.2. Discuss

Few studies conducted prior to this study using imbalanced datasets. In general, when modeling imbalanced data, the model may fail to generalize, or the model may be biased towards classes with a large number of data. Therefore, in this study, the dataset situation when people face an unknown virus for the first time is restored. In the comparison test, it shows that adding the BN layer and the Dropout layer dramatically improves the accuracy, and it is desirable to use a deeper VGG-19. However, the proposed BND-VGG-19 also has limitations. From the experimental results, the category performance of COVID-19 is inferior to the other two categories' performance. Thus the generalization ability of the algorithm still has spaces for improving.

Table 6
Compare the proposed COVID-19 diagnostic method with other methods.

NO.	Study	Type of images	Number of cases	Method used	Accuracy (%)
1	Wang et al. [22]	X-ray	53 COVID-19 5526 Pneumonia 8066 Healthy	COVID-Net	92.40
2	Xu et al. [23]	CT	219 COVID-19 224 Pneumonia 758 Normal	ResNet + Location Attention	86.07
3	El Asnaoui & Chawki [24]	X-ray & CT	1493 COVID-19 2780 Pneumonia 1538 Normal	Inception_Resnet_V2 DensNet201 Resnet50 Mobilent_V2 Inception_V3 VGG-16	92.18 88.09 87.54 85.47 88.03 74.84
4	Ozturk et al. [25]	X-ray	125 COVID-19 500 Pneumonia 500 Normal	DarkCovidNet	87.02
5	Perumal et al. [26]	X-ray & CT	2538 COVID-19 1345 Pneumonia 1349 Normal	Haralick+ VGG16, Resnet50 Inception V3	93.80 89.20 82.40
6	Elzeki et al. [27]	X-ray	2210 COVID-19 2340 Pneumonia 1480 Normal	CXRVN	93.07
7	MAHMUD et al. [28]	X-ray	305 COVID-19 305 Pneumonia 305 Normal	CovXNet	89.6
8	Yang N et al. [29]	X-ray	COVID-19 Pneumonia Normal	GLCM + SVM GLRLM + SVM NGLDM + SVM GLZLM + SVM Histogram + SVM	85.95 83.80 80.65 79.25 81.65
9	Pham, Tuan D [30]	X-ray	COVID-19 Pneumonia Normal	Data augmentation + AlexNet Data augmentation + GoogleNet Data augmentation + SquzzezNet Data augmentation + ShuffleNet Data augmentation + NasNet-Mobile Data augmentation + NasNet-Large	74.50 ± 4.40 78.97 ± 3.70 78.52 ± 7.56 86.13 ± 10.16 83.45 ± 7.36 85.23 ± 8.25
10	Song et al. [31]	CT	777 COVID-19 505 Pneumonia 708 Normal	ARENET	93.00
11	Toraman et al. [32]	X-ray	COVID-19 Pneumonia Normal	CapsNet	84.22
12	Pham [33]	X-ray	438 COVID-19 438 Pneumonia 438 Normal	AlexNet+Dl GoogleNet+Dl SqueezeNet+DL	96.46 96.20 96.25
13	Dalia Yousri et al. [11]	X-ray	134 COVID-19 500 Pneumonia 500 Normal	FO-CS(ml)	84.67
14	Proposed Study	X-ray	219 COVID-19 1300 Pneumonia 1300 Normal	BND-VGG-19	95.48

6. Conclusion and future work

As of today, the COVID-19 virus continues spreading, the number of infections is rising, and hospital workloads has spaces for improving, and experts worldwide are still working together to collect data and study possible treatment options. One of the most urgent during this global pandemic is the detection of suspected cases requires further hospital testing to confirm infection. To break through this bottleneck, doctors are stepping up the development of diagnostic tests that are not yet routinely used. Therefore, this paper proposed a deep learning convolutional neural network for detection and identification based on chest X-rays to determine whether the infection is COVID-19, viral pneumonia, or normal.

In this paper, the BND-VGG-19 method was used to measure chest X-ray images, which belongs to the three-category method. The experiment used two GPUs and took only forty minutes to train for 40 epochs. Compared with other algorithms, the network's complexity and time calculation cost are efficient. The experimental results showed that using the BND-VGG-19 method, and the accuracy rate reaches 95.48%. The experimental result of BND-VGG-16 is only 81.10%. In future experiments, we shall consider the dynamic balance between accuracy maximization and the number of network layers when deepening

Table 7
Comparison of this method with other methods containing VGG-19 (3-Class).

NO.	Study	Type of images	Number of cases	Method used	Accuracy (%)
1	Apostolopoulos & Mpesiana [16]	X-ray	224 COVID-19 700 Pneumonia 504 Normal	Transfer learning + VGG-19	93.48
2	Fayemiwo et al. [34]	X-ray	1300 COVID-19 1300 Pneumonia 1300 Normal	DTL + VGG-19	92.92
4	Sitaula et al. [35]	X-ray	COVID-19 Pneumonia Normal	MBoDVW + VGG-16	84.37
5	Horry et al. [17]	X-ray	130 COVID-19 140 Pneumonia 400 Normal	VGG-19	87.00
6	Rahaman et al. [36]	X-ray	260 COVID-19 300 Pneumonia 300 Normal	Transfer learning + VGG-19	89.30
7	El Asnaoui K & Chawki Y [24]	X-ray & CT	1493 COVID-19 2780 Pneumonia 1538 Normal	VGG-19	72.52
8	Pham, Tuan D [30]	X-ray	COVID-19 Pneumonia Normal	Data augmentation VGG-19	83.22 ± 5.85
9	Proposed Study	X-ray	219 COVID-19 1300 Pneumonia 1300 Normal	BND-VGG-19	95.48

the number of network layers. In addition, there is still room for improving accuracy, such as further optimization to improve the study's accuracy when encountering larger datasets. Future research will use chest CT scans to construct more sensitive diagnostic modalities. While obtaining many professional medical photos, the method can also be used to detect other diseases, thereby improving the recognition efficiency as early as possible and reducing the workload of doctors.

CRediT authorship contribution statement

Zili Cao: Data curation, Writing – original draft. **Junjian Huang:** Conceptualization, Writing – reviewing & editing. **Xing He:** Writing – reviewing & editing. **Zhaowen Zong:** Writing – reviewing & editing.

Declaration of competing interest

The authors declare that they have no known competing financial interests or personal relationships that could have appeared to influence the work reported in this paper.

Data availability

No data was used for the research described in the article.

Acknowledgments

This work is supported by the Fundamental Research for the Central Universities, China (Project No. SWU020005).

References

[1] WHO, Report of the WHO-China Joint Mission on Coronavirus Disease 2019 (COVID-19), World Health Organization, 2020.
[2] Chinese medical journa, Diagnosis and treatment protocol for novel coronavirus pneumonia (trial version 7), Chinese Med. J. (2020) 1087–1095.
[3] T. Ai, Z. Yang, H. Hou, et al., Correlation of chest CT and RT-PCR testing in coronavirus disease 2019 (COVID-19) in China: A report of 1014 cases, Radiology (2020) 200642.
[4] Y. Li, S. Zhang, L. Guo, et al., NetNMSP: Nonoverlapping maximal sequential pattern mining, Appl. Intell. 52 (9) (2022) 9861–9884.
[5] Ozturk. T, Talo. M, et al., Automated detection of COVID-19 cases using deep neural networks with X-ray images, Comput. Biol. Med. (2020) 121–103792.
[6] P.K. Sethy, K. Santi, Behera, et al., Detection of coronavirus disease (COVID-19) based on deep features, Int. J. Math. Eng. Manage. Sci. (2020) 643–651.
[7] Y. Wu, Q. Hu, Y. Li, et al., OPP-miner: Order-preserving sequential pattern mining, 2022, arXiv e-prints.
[8] R.M. Pereira, D. Bertolini, L.O. Teixeira, et al., COVID-19 identification in chest X-ray images on flat and hierarchical classification scenarios, Comput. Methods and Prog. Biomed. 194 (2020) 105–532.
[9] A.S. Ashour, M.M. Eissa, M.A. Wahba, et al., Ensemble-based bag of features for automated classification of normal and COVID-19 CXR images, Biomed. Signal Process. Control (2021) 102–656.
[10] Widodo. CS, Naba. A, et al., UBNet: Deep learning-based approach for automatic X-ray image detection of pneumonia and COVID-19 patients, X-Ray Sci. Technol. (2022) 57–71.
[11] D. Yousri, M. Elaziz, L. Abualigah, et al., COVID-19 X-ray images classification based on enhanced fractional-order cuckoo search optimizer using heavy-tailed distributions, Appl. Soft Comput. 101 (3) (2021) 107–052.
[12] S. Toraman, T.B. Alakus, I. Turkoglu, Convolutional capsnet: A novel artificial neural network approach to detect COVID-19 disease from X-ray images using capsule networks, Chaos Solitons Fractals 140 (2020) 110–122.
[13] D. Das, K.C. Santosh, U. Pal, Truncated inception net: COVID-19 outbreak screening using chest X-rays, Phys. Eng. Sci. Med. 43 (10223) (2020).
[14] A.M. Hasan, M.M. Aljawad, H.A. Jalab, et al., Classification of Covid-19 coronavirus, pneumonia and healthy lungs in CT scans using Q-deformed entropy and deep learning features, Entropy 22 (5) (2000) 517.
[15] J. Sun, X. Li, C. Tang, et al., MFBCNNC: Momentum factor biogeography convolutional neural network for COVID-19 detection via chest X-ray images, Knowl.-Based Syst. 232 (2021) 107494.
[16] ID. Apostolopoulos, TA. Mpesiana, Covid-19: automatic detection from X-ray images utilizing transfer learning with convolutional neural networks, Phys. Eng. Sci. Med. (2020) 635–640.
[17] M.J. Horry, S. Chakraborty, M. Paul, et al., COVID-19 detection through transfer learning using multimodal imaging data, IEEE Access 99 (2020) 1.
[18] S. Ioffe, C. Szegedy, Batch Normalization: Accelerating Deep Network Training By Reducing Internal Covariate Shift, JMLR.org, 2015, pp. 448–456.
[19] N. Srivastava, G. Hinton, A. Krizhevsky, et al., BDropout: A simple way to prevent neural networks from overfitting, J. Mach. Learn. Res. 15 (1) (2014) 1929–1958.
[20] M. Pavlova, N. Terhljan, A.G. Chung, et al., COVID-Net CXR-2: An enhanced deep convolutional neural network design for detection of COVID-19 cases from chest X-ray images, 2021, arXiv:2105.06640.

[21] K. Simonyan, A. Zisserman, Very deep convolutional networks for large-scale image recognition, 2014, arXiv:1409.1556.
[22] L. Wang, Z.Q. Lin, A. Wong, COVID-Net: A tailored deep convolutional neural network design for detection of COVID-19 cases from chest X-ray images, Sci. Rep. (2020) 19549.
[23] X. Xu, X. Jiang, C. Ma, et al., Deep learning system to screen coronavirus disease 2019 pneumonia, 2020, arXiv:2002.09334.
[24] K.El. Asnaoui, Y. Chawki, Using X-ray images and deep learning for automated detection of coronavirus disease, Biomol. Struct. Dyn. (2021) 3615–3626, PMID: 32397844.
[25] T. Ozturk, M. Talo, EA. Yildirim, et al., Automated detection of COVID-19 cases using deep neural networks with X-ray images, Comput. Biol. Med. (2020) 121–103792.
[26] V. Perumal, V. Narayanan, S.J.S. Rajasekar, Detection of COVID-19 using CXR and CT images using transfer learning and Haralick features, Appl. Intell. (2020) 1–18.
[27] O.M. Elzeki, M. Shams, S. Sarhan, et al., COVID-19: a new deep learning computer-aided model for classification, PeerJ Comput. Sci. 7 (1) (2021) e358.
[28] M. Tanvir, AR. Md, AF. Shaikh, CovXNet: A multi-dilation convolutional neural network for automatic COVID-19 and other pneumonia detection from chest X-ray images with transferable multi-receptive feature optimization, Comput. Biol. Med. (2020) 103869.
[29] N. Yang, F. Liu, C. Li, et al., Diagnostic classification of coronavirus disease 2019 (COVID-19) and other pneumonias using radiomics features in CT chest images, Sci. Rep. (2021) (2019).
[30] D.Pham. Tuan, Classification of COVID-19 chest X-rays with deep learning: new models or fine tuning? IEEE Access (2021) 2047–2501.
[31] Y. Song, S. Zheng, L. Li, et al., Deep learning enables accurate diagnosis of novel coronavirus (COVID-19) with CT images, IEEE/ACM Trans. Comput. Biol. Bioinform. (2021) 2775–2780.
[32] S. Toraman, T.B. Alakus, I. Turkoglu, Convolutional capsnet: A novel artificial neural network approach to detect COVID-19 disease from X-ray images using capsule networks, Chaos Solitons Fractals 140 (2020) 110122.
[33] T.D. Pham, A comprehensive study on classification of COVID-19 on computed tomography with pretrained convolutional neural networks, Sci. Rep. (2020) 2045–2322.
[34] M.A. Fayemiwo, T.A. Olowookere, Arekete.S.A. and, et al., Modeling a deep transfer learning framework for the classification of COVID-19 radiology dataset, 2PeerJ Comput. Sci. (2021) e614.
[35] C. Sitaula, T.B. Shahi, S. Aryal, et al., Fusion of multi-scale bag of deep visual words features of chest X-ray images to detect COVID-19 infection, Sci. Rep. 11 (1) (2021) 1–12.
[36] M.M. Rahaman, C. Li, Y. Yao, et al., Identification of COVID-19 samples from chest X-ray images using deep learning: A comparison of transfer learning approaches, J. X-Ray Sci. Technol. 28 (5) (2020) 821–839.